Experimental Flow Studies on Carotid Artery Models with and without Stents

Liepsch, D [1], Schmid, Th.[1], Klügel, G.[1], Sakurai, A.[3], Berger, H.[2], Greil, O.[2]

[1] FB 05, Fachhochschule München, Lothstr. 34, D-80335, Munich, Germany

[2] Klinikum rechts der Isar, TU München, Ismaningerstr. 22, D-81675, Munich, Germany

[3] Kansai University Suita, Osaka, Japan

Abstract

For patients at high risk due to stenosis, placement of stents in the carotid artery is a preferred treatment. However, stents often cause flow disturbances leading to clotting and re-stenosis in such patients. Therefore we studied the flow behavior of a covered stent, placed in a carotid artery at two different positions and compared these with the measurements carried out in a carotid model without stent. The covered stents were positioned from the common carotid artery into the internal carotid artery (ICA). The changes in flow rate and velocity distribution were measured with a laser Doppler anemometer. The results show that the stent changed the flow, especially in the external carotid artery (ECA). The velocity pattern at the entry of the stent was not significantly affected nor was the post-stent region in the ICA. However, changes in the velocity distribution were observed in the ECA, influenced by the mesh structure of the implanted stents. These studies can be useful for improving stent design and in its clinical applications, by indicating optimal positions for stent placement.

1. Introduction

Biofluid mechanical studies are important for the evaluation of diagnostic and therapeutic procedures. The role of the flow pattern in atherosclerosis is well known. Disturbances to the normal physiological flow can influence biological function of cells. It is, therefore, important to determine what influence, if any, surgical procedures and measuring techniques may have upon the flow behavior. Many studies in bends and bifurcations have been done. Investigations into the optimal anastomosis angle and the placement of heart valves have also been performed. In this paper, we present some applications of biofluid mechanical studies to the testing of stent placement in cardiac patients.

The implantation of stent in carotid arteries is controversial. Patients in with serious cardiac deficiency or with complicated local conditions in the throat area after surgery or angiographic investigation should not undergo a surgical procedure (endarterectomy). In such cases stent implantations are an alternative.

We studied three different stent types at various positions in the in carotid arteries to determine which would be the most effective and safe. Our findings were compared with the flow of healthy carotid artery models without stent.

2. Models

We used physiological models of the carotid artery with bifurcation angles of 37 between internal carotid artery (ICA and external (ECA).

- Model 1: A Schneider wall stent 7 mm diameter, 15 mm in length, was placed entirely in the ICA.
- Model 2: A Schneider wall stent, 6 mm diameter, 15 mm in length, in the ICA and in the bulb of the carotid artery.
- Model 3: A Schneider wall stent, 9 mm diameter, 25 mm in length, in the common carotid artery (CCA) and ICA.

3. Experimental set up and measurements methods

The flow was visualized with dyes under steady flow conditions and with a photoelasticity apparatus using a birefringent solution under pulsatile flow conditions. These methods are only qualitative. They do, however, show where the flow is disturbed, where vorticities arise, the elongation of such vorticities and flow separation regions. These areas were then investigated.

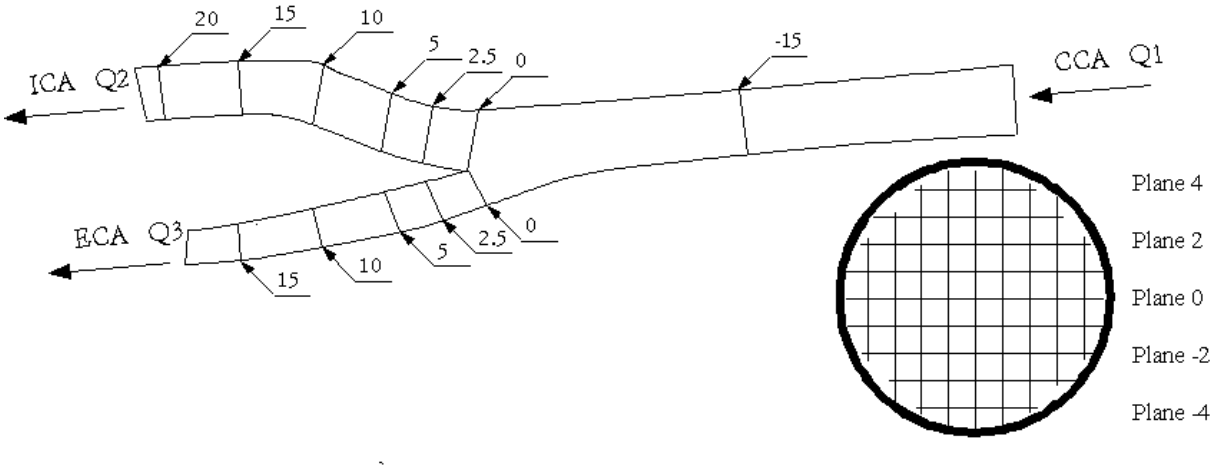

Fig. 1. Planes and positions for LDA measurements.

For quantitative values we used a one-component He-Ne laser-Doppler-anemometer (LDA) (BBC Goerz) 5 mW, wavelength λ= 632.8 mm. Figure 1 shows the positions and planes of the LDA measurements under pulsatile flow conditions with a frequency of 60 pulses per minute. The flow in the common carotid artery was 25.8 l/h or a Reynolds number of Re = 250. This Reynolds number is an average calculated over one pulse cycle. The local velocity was measured at each point for eight pulse cycles. In each plane, 85 points were measured. The velocity curve in the CCA and pressure curve is shown in Figure 2.

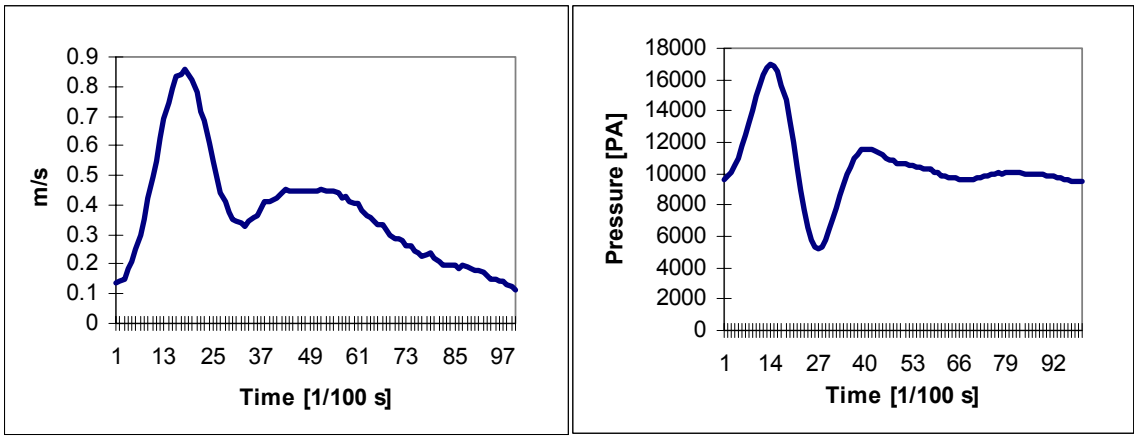

Fig. 2 Velocity and pressure curve at the entrance of the common carotid artery model.

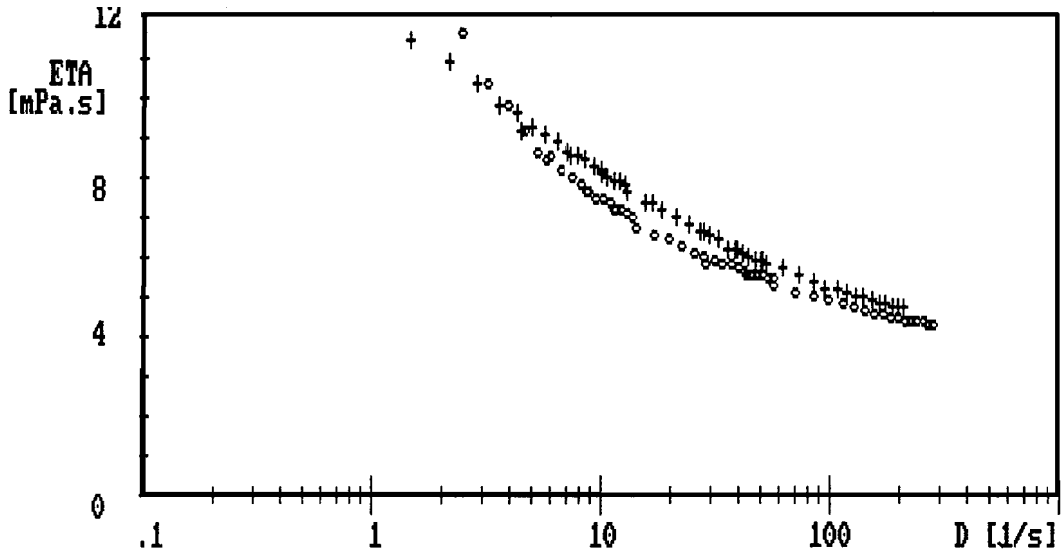

Fig. 3. Comparison between human blood viscosity (oooo) and the model fluid (++++).

All experiments were done under physiological flow conditions. It was not possible to use human blood because the laser light would have been absorbed. Therefore, we used a blood-like fluid developed in our laboratory. This fluid is a dimethylsulfoxide-water mixture to which a polyacrylamide water solution is added. This fluid has a flow behavior similar to that of blood (Fig. 3). The apparent viscosity, as well as the elastic and viscous components of the model fluid, was nearly the same as the rheological behavior of human blood. The experimental set up is shown in Fig 4. for the LDA measurements, pressure and flow measurements.

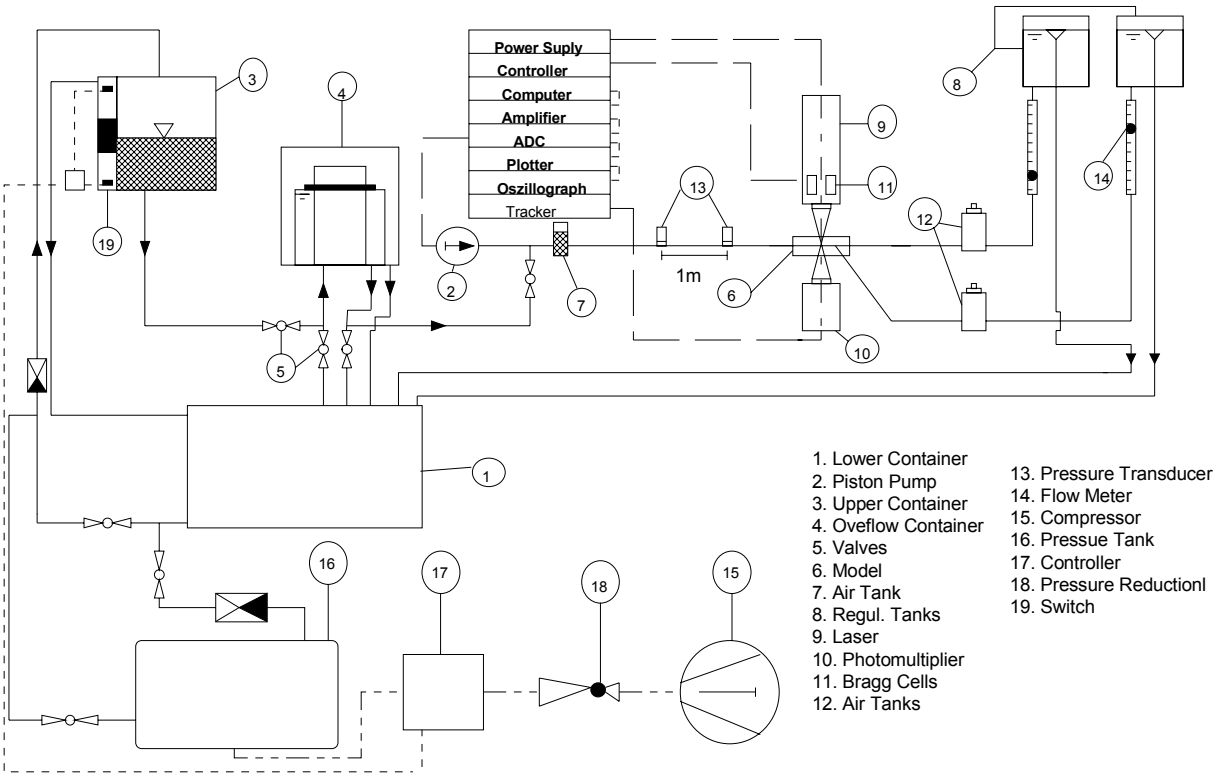

Fig. 4. Experimental set up

4. Results

Figure 5 shows the axial velocity distribution over one pulse cycle 5 mm downstream of the apex in the ICA at different phase angles. The average Re-number in the CCA was Re = 250 and the Womersley parameter α = 3.85. The flow rate ratio between the internal and external carotid artery was 70.3: 29.7. A large flow separation region can be seen at phase 90°, just after the peak velocity of the systolic phase. The highest velocity values are found at the inner wall side. The flow separation region extends over nearly three-quarters of the whole cross section and slowly decreases during the diastolic phase.

Figure 6 shows a comparison of between the carotid artery model without stent and the three different models with the stents at a phase angle of 60°, the peak systolic phase. The distance was 5 mm distal to the apex in the ICA. Stent 2 shows much larger velocity disturbances than Stent 3. Smaller disturbances are also seen in Stent 1. Figure 7 shows the same comparison 15 mm distal to the apex in the ICA. Here Stent 1, of course, does not influence the velocity distribution, whereas Stent 3 has a significant effect on the velocity distribution.

We found the following: In Stent 1 the flow rate ratio ICA/ECA (with stent) remained at 70.9/29.1, largely unchanged from 70.3/29.7 without the stent. Proximal to the stent in the separation zone there was a systolic velocity increase. During the diastolic phase, a minimal velocity decrease was apparent. The velocity within the stent increased during systole up to 0.19 m/sec. The separation zone can be clearly seen. Ten mm into the stent, the profile normalized. Five mm and 10 mm distal to the stent there was a velocity decrease (0.1 m/s) towards the inner wall.

In Stent 2 the flow rate ratio ICA/ECA changed from 70.3/29.7 in the model without stent to 75.1/24.9 caused by the narrow mesh grid of the stent. The peak velocities were about 0.46 m/s higher at the stent. The velocity was higher through the entire pulse cycle. Velocities close to the wall distal to the stent are lower compared to the model without stent. Five mm and 10 mm distal to the stent, the velocity profiles are altered including small vortices. Significant velocity disturbances can be seen in the ECA. These remain up to 20 mm downstream of the apex. The velocity in the local separation region is about 0.41 m/s higher than in the model without stent. The backward flow found in the bulbus of the model without stent disappears in the model with stent. The stent act as a grid in the ECA equalizing the velocity over the cross-section, as is found in tubes with grids.

In Stent 3 the flow rate ratio changed from 70.3/29.7 in the model without stent to 72.4/27.6 with stent. The grid of the stent increased the flow resistance, especially at the entrance of the ECA. The stent acts as a large mesh grid.

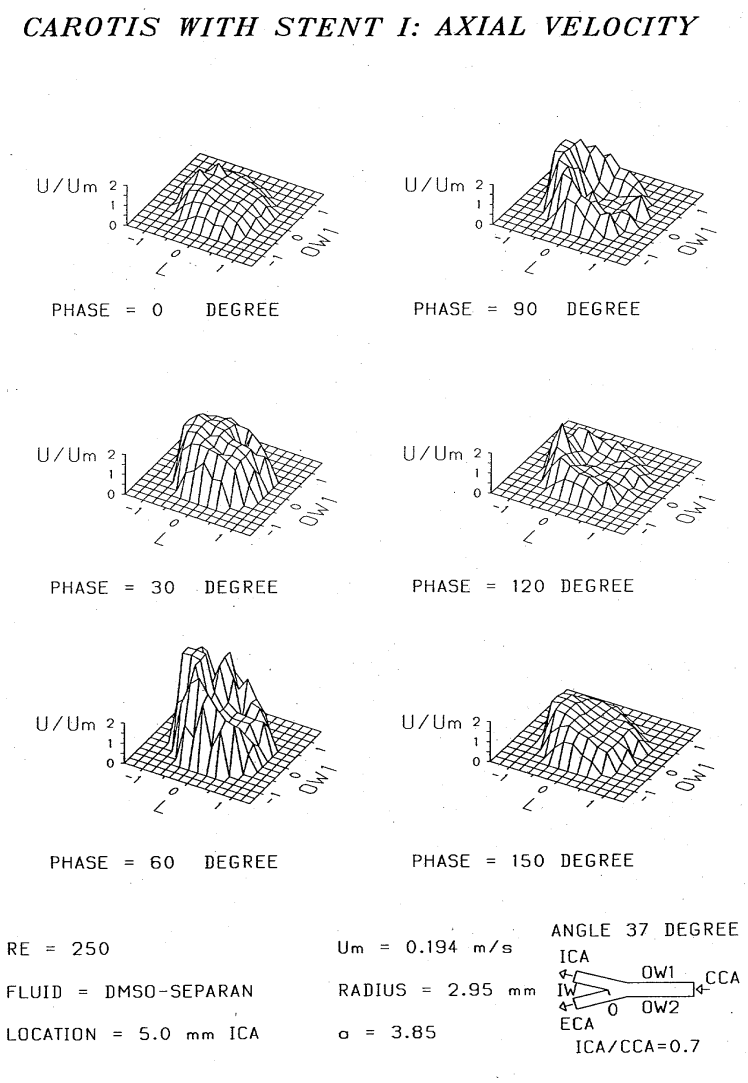

Fig. 5. Velocity distribution (of the axial velocity component) at different phase angles for plane 5 mm downstream of the apex in the ICA with Stent I.

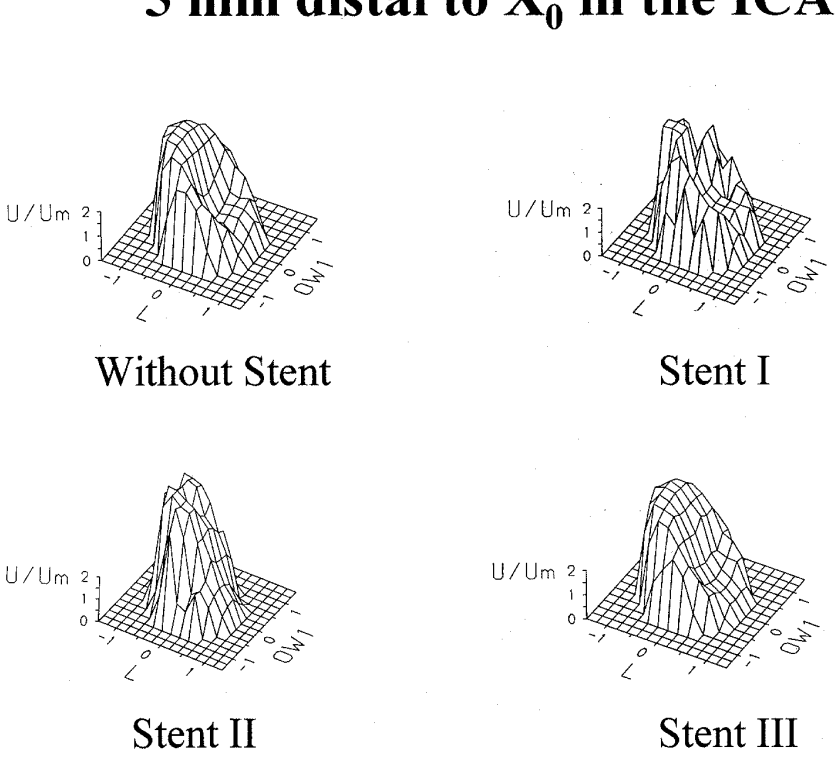

Fig. 6. Velocity distribution in the ICA 5 mm distal to the apex without stent and the three different types of stents.

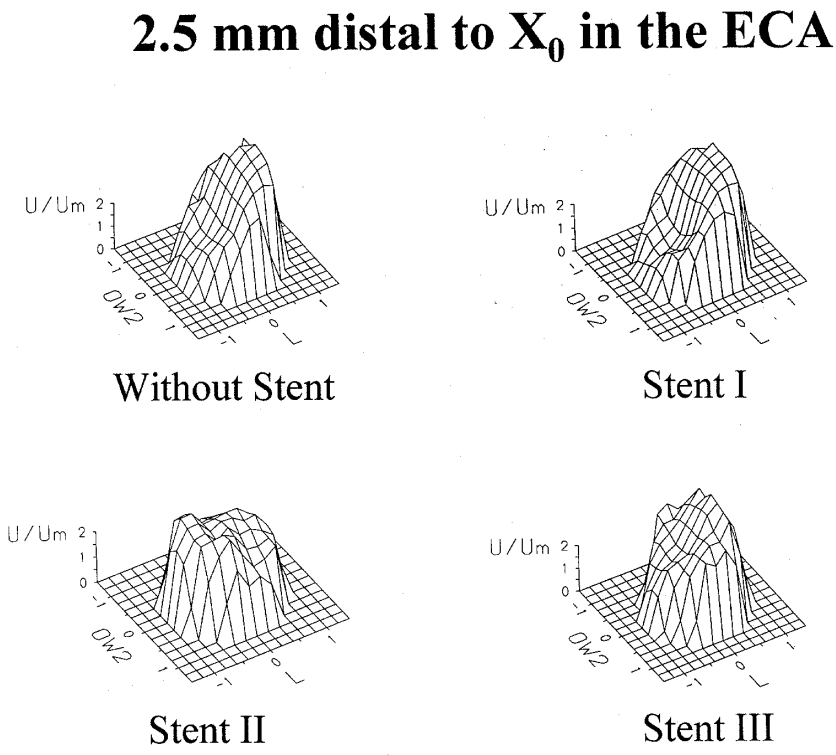

Fig. 7. Same as Fig. 6 2.5 mm distal to the apex in the external carotid artery.

Figure 8 shows the velocity distribution of two covered stents in comparison with a carotid artery without stent. The flow in the External carotid artery is totally changed caused by the covered area of the stents.

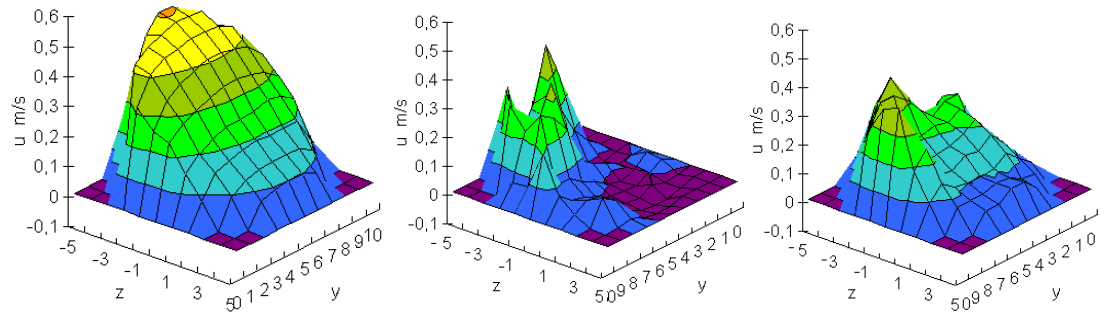

empty stent 1 stent 2

(a) T=20 at position F

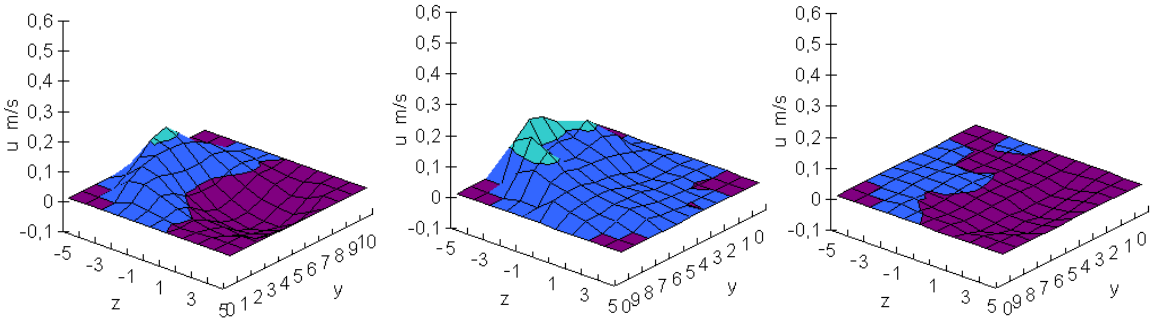

empty stent 1 stent 2

(b) T=40 at position F

Figure 8 Velocity distributions in the model without stent and in models with covered stents at different positions at phase (a) ωt= 72 ° (systolic peak) and (b) ωt=144 ° (diastolic period). The flow in the CCA was Re=250. The measured plane in ECA is 0mm distal to the bifurcation.

5. Summary and Conclusion

The flow pattern of Model 1 showed almost no variations from the physiological flow in the carotid. When the ECA is bridged by a large mesh grid (Model 3), the flow in the ICA remains undisturbed. In the ECA, the flow separation zone doesn't appear. Stent 2, on the other hand, is very dangerous. In the ICA dead zones occur directly behind the stent.

Implantation of a stent near the carotid artery can lead to risk of thrombosis or re-stenosis. Stents may, however, be less risky than endarterectomy for patients in extremely bad health.

Physicians have to be trained carefully, because it is important to place the stent very precisely. This can be done with models reducing animal studies. Many questions

remain as to the influence of the stent on the elasticity of the vessel wall, the interaction of the blood and the endothelial cell layer and blood clotting mechanism.

6. Acknowledgement

We want to thank the DFG for their support of this project.